JOURNAL OF MATERIALS SCIENCE **40** (2005) 5125–5131

Electrical properties of V_2O_5-CaO-P_2O_5 glasses exhibiting majority charge carrier reversal

B. I. SHARMA*, A. SRINIVASAN‡
Physics Department, Indian Institute of Technology Guwahati, Guwahati-781039, India
E-mail: asrini@iitg.ernet.in

The thermoelectric power and d.c electrical conductivity of $x\,V_2O_5{\cdot}40CaO{\cdot}(60-x)P_2O_5$ ($10 \leq x \leq 30$) glasses were measured. The Seebeck coefficient (Q) varied from $+88\ \mu V\ K^{-1}$ to $-93\ \mu V\ K^{-1}$ as a function of V_2O_5 mol%. Glasses with 10 and 15 mol% V_2O_5 exhibited *p*-type conduction and glasses with 25 and 30 mol% V_2O_5 exhibited *n*-type conduction. The majority charge carrier reversal occurred at $x = 20$ mol% V_2O_5. The variation of Q was interpreted in terms of the variation in vanadium ion ratio (V^{5+}/V^{4+}). d.c electrical conduction in $x\,V_2O_5{\cdot}40CaO{\cdot}(60-x)P_2O_5$ ($10 \leq x \leq 30$) glasses was studied in the temperature range of 150 to 480 K. All the glass compositions exhibited a cross over from small polaron hopping (SPH) to variable range hopping (VRH) conduction mechanism. Mott parameter analysis of the low temperature data gave values for the density of states at Fermi level $N(E_F)$ between 1.7×10^{26} and $3.9 \times 10^{26}\ m^{-3}\ eV^{-1}$ at 230 K and hopping distance for VRH (R_{VRH}) between 3.8×10^{-9}m to 3.4×10^{-9} m. The disorder energy was found to vary between 0.02 and 0.03 eV. $N(E_F)$ and R_{VRH} exhibit an interesting composition dependence. © *2005 Springer Science + Business Media, Inc.*

1. Introduction

Ever since Denton *et al.* [1] reported that systems containing V_2O_5 as one of the components form semiconducting glasses, a variety of semiconducting oxide glasses has been reported. Glassy semiconductors are obtained when melts containing transition metal oxides such as V_2O_5 and a wide range of oxides like P_2O_5, TeO_2, GeO_2 [2, 3] etc., are quenched. V_2O_5–P_2O_5 glasses have attracted a lot of attention [3–6] due to their high electrical conductivity. The presence of vanadium in two valence states, namely, V^{4+} and V^{5+} influences the electrical conduction mechanism in these glasses [7–9]. The electrical conduction in these glasses has been attributed [9–11] to hopping of electrons from an ion of low valence state (V^{4+}) transition metal to an ion of high valence state (V^{5+}). The Mott-Austin small polaron hopping model [9, 12, 13] has been widely used for interpreting the electrical conduction mechanism in these glasses. d.c conductivity of V_2O_5–Bi_2O_3 [10] and V_2O_5–TeO_2 [13] glasses have been reported. Vanadium phosphate glasses generally exhibit *n*-type semiconductor behaviour [4–6, 9]. In their pioneering work, Kennedy *et al.* [2] reported the possibility of obtaining a *p*-type composition in $x\,V_2O_5{\cdot}40CaO{\cdot}(60-x)P_2O_5$ glasses [2], namely, $10V_2O_5{\cdot}40CaO{\cdot}50P_2O_5$. They also reported the high temperature electrical conductivity data of $x\,V_2O_5{\cdot}40CaO{\cdot}(60-x)P_2O_5$ ($10 \leq x \leq 30$) glasses. In the present work, a detailed study of the d.c. conduction mechanism in $x\,V_2O_5{\cdot}40CaO{\cdot}(60-x)P_2O_5$ ($10 \leq x \leq 30$) glasses has been carried out over a wide range of temperature (150 to 480 K) with a view to understand conduction mechanism in these glasses. The majority charge carrier reversal occurring in these glasses has been studied using thermoelectric power measurements and vanadium ion ratio.

2. Experimental

Glass samples of the system $x\,V_2O_5{\cdot}40CaO{\cdot}(60-x)P_2O_5$ ($10 \leq x \leq 30$) were prepared by the melt quenching technique. Appropriate amounts of high purity V_2O_5, $CaCO_3$ and P_2O_5 were thoroughly mixed by continuously kneading for about 15 to 20 min. The mixture was then transferred to an alumina crucible and melt at about 1100°C in an electric furnace. The overall weight of the mixture was about 3 gm per batch. The melt was held at this temperature for about 3 to 4 h before press quenching the same by pouring it between two copper plates. The as-quenched samples were in the form of platelets of about 1 mm thickness. The amorphous nature of the as-quenched samples was verified using the X-ray diffraction technique. The glassy nature of the samples was confirmed from the observation of the glass transition temperature (T_g) from the differential scanning calorimeter (DSC) curves. The glass transition temperature of the as-quenched samples varied between 400 and 500 K. The thermoelectric power (TEP) measurements were performed on a thin slice of

Present address: Physics Department, Assam University, Silchar, Assam-788011, India.
‡Author to whom all correspondence should be addressed.
0022–2461
DOI: 10.1007/s10853-005-4401-6

TABLE I Seebeck coefficient Q (experimental and calculated), vanadium ion ratio, activation energy for thermopower ΔE_s, (data given in brackets were taken from ref. [2])

Composition (mol%) V_2O_5:CaO:P_2O_5	Q (expt.) (μVK^{-1})	Q (from equation 5) (μVK^{-1})	c V^{4+}/V^{tot}	V^{5+}/V^{4+}	ΔE_s (meV)
10:40:50	+88	+90	0.735	0.36 (0.3)	0.88
15:40:45	+40	+31	0.588	0.70 (–)	0.77
20:40:40	0	0	0.5	1.0 (1.0)	—
25:40:35	−82	−80	0.284	2.52 (–)	0.70
30:40:30	−93	−88	0.264	2.79 (2.9)	0.61

glass sample, the details of which are given elsewhere [14]. Since the resistance of the as-quenched glass samples varied between 10^9 ohms and 10^3 ohms in the temperature range of 150 to 480 K, both collinear two-point probe and collinear four-point probe methods were employed to determine the d.c electrical conductivity of these glasses. The measurements were performed with an Electrometer (Keithley, model 6512) and a constant current source (Keithley, model 224) connected to an indigenously fabricated cryostat [15]. A spring-loaded four-point copper probe assembly was used to make electrical contact with the sample. Current used in the dc conductivity measurements was ∼50 nA, which is estimated to produce an electric field of the order of a few mV/m at 480 K. This field is very low to induce polarization effects and hence contribution to ionic conduction could be ignored. The concentration of V^{4+} and V^{5+} ions in the as-quenched glass samples used in the present studies was determined by iodometric titration [16]. The ratio of high valence to low valence vanadium ions, V^{5+}/V^{4+} determined are given in Table I. The density of the glass samples was determined using the Archimedes principle with xylene as the immersion liquid. The reported density data (Table I) is the average of at least three independent measurements.

3. Results and discussion

3.1. Thermoelectric power

The variation of thermoelectric power (Seebeck coefficient) with temperature T of semiconducting oxide glasses generally follows the relation [17],

$$Q = \pm\frac{k}{e}\left(\frac{\Delta E_s}{kT} + A\right) \tag{1}$$

where the positive and negative signs denote p-type and n-type conduction respectively, e is the electronic charge, k is the Boltzmann constant, T the absolute temperature, ΔE_s the activation energy for thermopower and A is a constant dependent on the mechanism of the electrical transport. The variation of the thermoelectric power (Seebeck coefficient) for the $x\text{V}_2\text{O}_5{\cdot}40\text{CaO}{\cdot}(60-x)\text{P}_2\text{O}_5$ where $10 \le x \le 30$ glasses is shown in Fig. 1. TEP data shown in Table I and Fig. 1 correspond to measurements made at 400 K. The solid line in the figure represents a least squares fit to the data. Heikes proposed [18, 19] that Q at high temperature (generally $T > 200$ K) is related to the fraction of reduced transition metal ion c by the expression,

$$Q = \left(\frac{k}{e}\right)\left\{\ln\left(\frac{c}{1-c}\right) + \alpha'\right\} \tag{2}$$

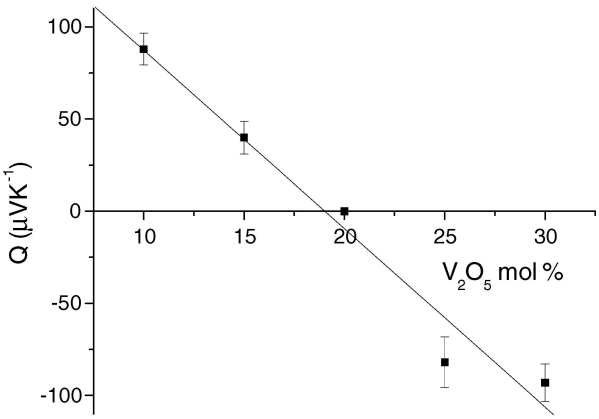

Figure 1 Variation of Seebeck coefficient Q (measured at 400 K) of $x\text{V}_2\text{O}_5{\cdot}40\text{CaO}{\cdot}(60-x)\text{P}_2\text{O}_5$ glasses with V_2O_5 mol%. Solid line is a least squares fit to the data.

where $c = V^{4+}/V^{\text{tot}}$, $V^{\text{tot}} = (V^{4+} + V^{5+})$ and α' is a constant (the ratio between heat transfer energy and the kinetic energy of carrier electrons). According to Austin and Mott [9] and Appel [20], $\alpha' \gg 2$ signifies large polaron hopping conduction mechanism and the conduction mechanism is due to small polaron hopping when $\alpha' < 1$. Equation 2 which is often referred to as Heikes law, can be rewritten as,

$$Q = \left(\frac{k}{e}\right)\ln\left(\frac{c}{1-c}\right) + \alpha'\left(\frac{k}{e}\right) \tag{3}$$

Equation 3 shows that the Q and $\ln(\frac{c}{1-c})$ should have a linear relation with a slope of k/e (= 86.18 μV/K) and a Y axis intercept equal to $\alpha'(\frac{k}{e})$. Fig. 2 shows the plot of experimental Q value and $\ln(\frac{c}{1-c})$ for the $x\text{V}_2\text{O}_5{\cdot}40\text{CaO}{\cdot}(60-x)\text{P}_2\text{O}_5$ glasses. The solid line shown in Fig. 2 is the least squares fit to the data. In the present case, the slope was found to be 89.62 μV/K, which was close to the expected value of k/e = 86.18 μV/K. Hence one can conclude that Heikes law is applicable to the present investigation of glasses within permitted experimental uncertainties. α' value estimated from the Y intercept of the least squares fit to be 0.0098. This is in reasonably good agreement with the value of 0.005–0.18 for the V_2O_5-CaO-P_2O_5 glasses as predicted by Kennedy and Mackenzie [2]. Consequently, the conduction mechanism in this system of glass is judged to be small polaron hopping considering the small values of $\alpha' < 1$.

According to Kennedy and Mackenzie [2], Q value of semiconducting transition metal oxide (TMO) glasses

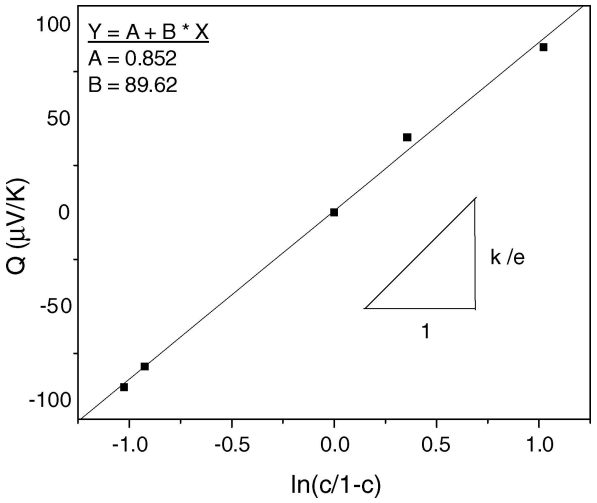

Figure 2 Relationship between $\ln(c/1-c)$ and Q for V_2O_5-CaO-P_2O_5 glasses at 400 K.

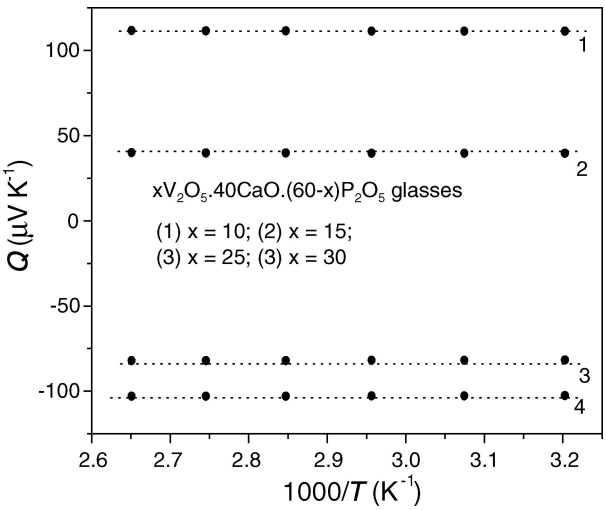

Figure 3 Q verses $1000/T$ for $xV_2O_5{\cdot}40CaO{\cdot}(60-x)P_2O_5$ ($10 \leq x \leq 30$) glasses. Dotted line corresponds to the least squares fit to the experimental data.

could be expressed in general as,

$$Q = \left(\frac{k}{e}\right) \ln \left[\frac{high\ valence\ ions}{low\ valence\ ions}\right] \tag{4}$$

In case of vanadate glasses, Equation 4 can be represented by the relation,

$$Q = \left(\frac{k}{e}\right) \ln \left(\frac{V^{5+}}{V^{4+}}\right) \tag{5}$$

Substitution of vanadium ion concentration estimated from iodometric titration [16] in the above relation yielded Q (calculated from Equation 5) values, which were comparable to the Q (expt.) values obtained from TEP measurements. Both the calculated and experimental Q values are tabulated in Table I. It can also be seen from the data presented in Table I that Q was negative (n-type semiconductor) for glasses with $(V^{5+}/V^{4+}) > 1$. Similarly, Q was positive (p-type semiconductor) for glasses with $(V^{5+}/V^{4+}) < 1$. Thus, glasses with 10 and 15 mol% V_2O_5 with corresponding (V^{5+}/V^{4+}) ratio values of 0.36 and 0.70 respectively are p-type glassy semiconductors. It is evident that the p-type conduction in these glasses is due to the predominance of the V^{4+} ion over V^{5+} ion. The n-type to p-type charge carrier reversal in these glasses is thus attributed to the change in relative concentration of the low and high valence vanadium ion.

Q verses $1000/T$ plots corresponding to various glass compositions are shown in Fig. 3. The dotted lines are the least squares fit to the data. Fig. 3 shows that Q exhibits a weak dependence on temperature. This weak T dependence of Q has been observed in other V_2O_5 based glasses [6] and appears to be a characteristic of this class of glassy semiconductors. Fig. 4 shows the variation of ΔE_s as a function of V_2O_5 mol%. The thermal activation energy decreases as V_2O_5 mol% increases. This indicates that the thermal conductivity of the glasses increases as V_2O_5 mol% is increased in $xV_2O_5{\cdot}40CaO{\cdot}(60-x)P_2O_5$ ($10 \leq x \leq 30$) glasses. A perceptible slope change in ΔE_s at $x = 20$ mol% V_2O_5 composition shows that the thermal conductivity undergoes an abrupt change at the MCCR composition. The inset in Fig. 4 shows the Q versus $1000/T$ plot for the $10V_2O_5{\cdot}40CaO{\cdot}50P_2O_5$ glass composition. The solid line corresponds to a least squares linear fit to the data.

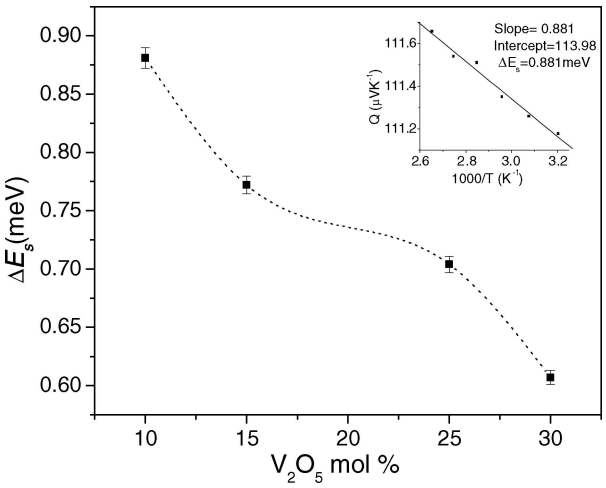

Figure 4 Activation energy for thermopower ΔE_s as a function of V_2O_5 mol% for $xV_2O_5{\cdot}40CaO{\cdot}(60-x)P_2O_5$ ($10 \leq x \leq 30$) glasses. Inset shows the variation of Q with 1000/T for a typical glass sample ($10V_2O_5{\cdot}40CaO{\cdot}50P_2O_5$).

3.2. d.c. electrical conductivity

3.2.1. High temperature regime

The high temperature electrical conductivity of amorphous semiconductors is described by the Mott and Austin relation [7, 21, 22], which is expressed as,

$$\sigma T = \sigma_o e^{-\frac{W}{kT}} \tag{6}$$

where W is the activation energy for conduction, T is the absolute temperature and k is the Boltzmann constant. The pre-exponential factor σ_o could be expressed as,

$$\sigma_o = \frac{c(1-c)\nu_o e^2}{Rk} e^{(-2\alpha R)} \tag{7}$$

TABLE II Glass density, density of metal ion sites N, average ion spacing R, activation energy for conduction W, (data given in brackets are from [2])

Composition (mol%) V_2O_5:CaO:P_2O_5	Density ($g \cdot cm^{-3}$)	N (10^{27} m^{-3})	R (10^{-10} m)	W (eV)
10:40:50	2.76 (2.799)	2.9	6.9	0.31
15:40:45	2.84 (–)	4.5	6.0	0.30
20:40:40	2.91 (2.963)	6.1	5.5	0.23
25:40:35	2.98 (–)	7.6	5.1	0.18
30:40:30	3.05 (3.052)	9.2	4.8	0.17

where, ν_o is the optical phonon frequency ($\sim 10^{11}$–10^{13} sec^{-1}), R the average spacing between transition metal ions, c the ratio of the amount of reduced transition metal ion to that of total transition metal ion, and α is the rate of wave function decay for the hopping electron. The average ion spacing R given by the relation,

$$R = \left(\frac{1}{N}\right)^{\frac{1}{3}} \tag{8}$$

where the N is the density of metal ion sites related to the glass density as,

$$N = 2\left[\text{density}\, x \left(\frac{\text{wt.}V_2O_5}{\text{Mol.wt.}V_2O_5}\right) N_A\right] \tag{9}$$

where wt.V_2O_5 is the wt. percentage of V_2O_5, Mol.wt. V_2O_5 is the molecular weight of V_2O_5 and N_A is the Avogadro's number The density of metal ion N was calculated using relation (9) and average ion spacing was estimated from relation (8) (Table II).

Fig. 5 shows the plot of $\ln(\sigma T)$ verses $1000/T$ for the glasses with different V_2O_5 mol%. The high temperature conductivity data in Fig. 5 shows a good fit to the relation (6) for all the samples (a typical fit for the glass with $x = 20$ mol% V_2O_5 is shown as an inset in Fig. 5), which confirms that the dominant conduction mechanism in this regime is small polaron hopping (SPH).

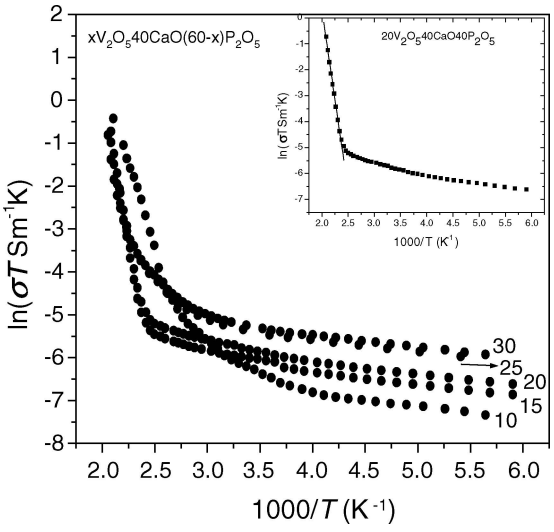

Figure 5 $\ln(\sigma T)$ verses $1000/T$ plots for $x V_2O_5 \cdot 40CaO \cdot (60 - x)P_2O_5$ glasses. Inset shows a typical fit of data to relation (3) (Every tenth data point has been plotted in order to improve the clarity of the figure).

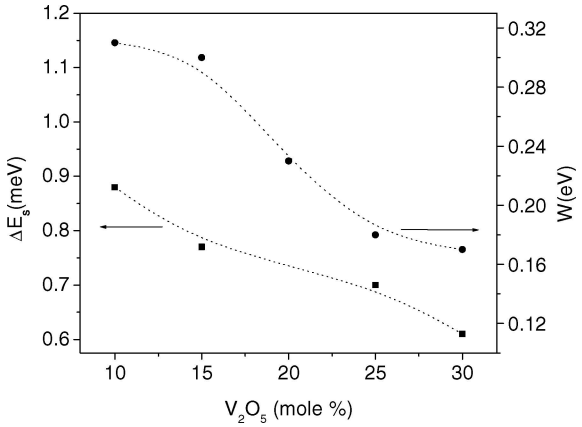

Figure 6 Activation energy for thermoelectric power ΔE_s and activation energy for high temperature d.c. conductivity W as a function of V_2O_5 mol% for $x V_2O_5 \cdot 40CaO \cdot (60 - x)P_2O_5$ ($10 \leq x \leq 30$) glasses.

The variation of W and ΔE_s with V_2O_5 mol% is shown in Fig. 6. The activation energy deduced from dc conductivity in the high temperature regime is greater than the thermoelectric power. The relative magnitude of W and ΔE_s indicates the predominant conduction mechanism in these glasses. It is evident from Fig. 6 that all glasses show the same type of conduction mechanism. There are several models which try to explain the difference in the magnitudes of W and ΔE_s. One such model by Emin [21] predicts that in glasses with $W > \Delta E_s$ a strong electron-phonon coupling exists, which results in the formation of small polarons. This notion is also supported by Heike's conclusion as discussed in the section on thermoelectric power of these glasses.

It can also be verified from Fig. 5 that all the $\ln(\sigma T)$ verses $1000/T$ curves show a slope change at some small range of temperature, there by indicating a deviation from the small polaron hopping mechanism described by relation (6). The observed slope change is due to the change over in the electrical conduction mechanism from SPH to VRH as one lowers the temperature [11, 23]. Such behaviour has also been observed in V_2O_5–Bi_2O_3 [10], V_2O_5–TeO_2 [13], and V_2O_5–SrO-Bi_2O_3 [24] glasses.

The small polaron hopping (SPH) conduction can be either adiabatic or non-adiabatic SPH. If the conduction is adiabatic, α in Equation 4 is negligible. Thus the term $e^{(-2\alpha R)}$ can be made approximately equal to unity and pre-exponential factor σ_o can be written as

$$\sigma_o = \frac{c(1-c)\nu_o e^2}{Rk} \tag{10}$$

Using the calculated values of σ_o (obtained from intercept of $\ln(\sigma T)$ verses $1000/T$ plot) and the values of c and R, the phonon frequency, ν_o is calculated using relation (10). It was found that the phonon frequency ν_o values ranged between 7.9×10^5 sec^{-1} and 5.2×10^7 sec^{-1}. The corresponding values of the Debye temperature T_θ ($h\nu_o/k$) turned out to be in the range between 0.00004 to 0.0025 K. These values for ν_o are unreasonable since the Debye temperature T_θ must be around 300 K (with a corresponding ν_o of $\sim 10^{13}$ sec^{-1}).

The small values of ν_o and T_θ give the evidence to the argument that adiabatic approximation is not applicable for the present case.

The same conclusions may be drawn from an alternate approach. According to Holstein [25], the temperature dependence of d.c conductivity is given by

$$\sigma = \left(\frac{\pi\, e^2 j^2}{R\, hkT}\right)\left[\left(\frac{\pi}{WkT}\right)\frac{\sinh\left(\frac{h\,\nu_o}{2kT}\right)}{\left(\frac{h\nu_o}{2kT}\right)}\right]^{\frac{1}{2}} e^{-\left(\frac{W+GW_P}{2kT}\right)} \tag{11}$$

where $W_p = 2W_H$, $W_H = W - W_D/2$ and $G = [\tan h(h\nu_o/2kT)]/(h\nu_o/2kT)$. W can be calculated from a linear fit to the conductivity data in high temperature region (above room temperature) from the $\ln(\sigma T)$ verses $1000/T$ plot (Fig. 5). It was observed that the activation energy for conduction W increases as the average ionic distance R increases (Fig. 6). The observed trend is as per theoretical prediction. For the estimation of W_H, W_D is needed. Generally $W_D < 0.1$ eV [25]. A report on V_2O_5-Sb_2O_3-TeO_2 glasses [26] provides a value of 0.01 eV for W_D and another on V_2O_5-P_2O_5 (88–49 mol% V_2O_5) glasses estimated $W_D <$ 0.1 eV [5]. Hence, one can assume $W_D = 0.01$ eV for $x\,V_2O_5{\cdot}40CaO{\cdot}(60-x)P_2O_5$ glasses. This enables one to approximately estimate W_H. j values were calculated from the Equation 11 using the conductivity data at a particular temperature. For SPH being adiabatic or non-adiabatic, the polaron bandwidth j must satisfy one of the following conditions, namely,

$$j > \Phi = (2kT\,W_H/\pi)^{1/4}(h\nu_o/\pi)^{1/2} \text{ adiabatic} \tag{12}$$
$$j < \Phi = (2kT\,W_H/\pi)^{1/4}(h\nu_o/\pi)^{1/2} \text{ nonadiabatic}$$

j value corresponding to each glass composition was calculated using Equation 11 taking $\nu_o = 10^{13}$ sec^{-1}. The j value calculated at 400 K varied from 3.4×10^{-4} eV to 1.8×10^{-5} eV and the corresponding Φ value was 0.03 eV. This showed that j was less than Φ for all the glasses. Thus, nonadiabatic SPH was the dominating conduction mechanism at high temperatures in all the glass compositions. Calculated j and Φ values are shown in Table III. The mobility μ for non-adiabatic in SPH [5] regime can be obtained from the relation,

$$\mu = \left(\frac{eR^2}{kT}\right)\left(\frac{1}{\hbar}\right)\left(\frac{\pi}{4W_H kT}\right)^{\frac{1}{2}} j^2 e^{-\frac{W}{kT}} \tag{13}$$

The mobility values estimated from Equation 13 are shown in Table III. Carrier concentration N_c in each glass composition as given by the relation,

$$\sigma = N_c\, e\, \mu \tag{14}$$

are listed in Table III.

3.2.2. Low temperature regime

In the low temperature region, Mott's treatment for variable range hopping [9] leads to a temperature dependence for the conductivity given by,

$$\sigma = B \exp\left(-A/T^{1/4}\right) \tag{15}$$

where A and B are parameters related to the localized wave function α, density of states at the Fermi energy $N(E_F)$, optical phonon frequency ν_o and the Boltzmann constant k, and are given by the expressions,

$$A = 2.06\left[\frac{\alpha^3}{k_N(E_F)}\right]^{\frac{1}{4}} \tag{16}$$

$$B = \left[\frac{e^2}{2\sqrt{8\pi}}\right]\nu_o\left[\frac{N(E_F)}{\alpha kT}\right]^{\frac{1}{2}} \tag{17}$$

Fig. 7 shows the $\ln(\sigma T^{1/2})$ verses $T^{-1/4}$ plots for glasses with $x = 10, 15, 20, 25$ and 30 mol% of V_2O_5 respectively. These plots highlight the temperature region over which the change over from SPH to VRH occurs in these glasses. As already mentioned, the slope change has been shown [9, 24] to be the signature of the conduction change from SPH to VRH. α and $N(E_F)$ were calculated from the slope and intercept values obtained from the linear fit to the low temperature data using the relations (16) and (17). For the occurrence of VRH conduction, the requirement $\alpha R_{\mathrm{VRH}} > 1$ and $W_d \leq kT$ (e.g., $W_d \leq 0.019$ eV at 230 K) should be satisfied. Evaluation of our data at 230 K gave αR_{VRH} values between 1.86 to 1.16 and W_d values ranging between 0.02 and 0.03 eV, which showed that the above criteria were satisfied. Hence the conduction mechanism in $x\,V_2O_5{\cdot}40CaO{\cdot}(60-x)P_2O_5$ ($10 \leq x \leq 30$) glasses in the low temperature range is attributable to VRH.

The hopping distance R_{VRH} in VRH regime and hopping energy W_o can be obtained from α and R_{VRH} values using the following relations [27, 28],

$$R_{\mathrm{VRH}} = \left[\frac{9}{(8\pi\alpha N(E_F)\,kT)}\right]^{\frac{1}{4}} \tag{18}$$

$$W_o = \frac{3}{\left(4\pi R_{\mathrm{VRH}}^3 N(E_F)\right)} \tag{19}$$

TABLE III Conductivity σ at 400 K, polaron band width j, the parameter Φ, carrier concentration N_c of $x\,V_2O_5{\cdot}40CaO{\cdot}(60-x)P_2O_5$ ($10 \leq x \leq 30$) glasses

Composition (mol%) V_2O:$_5$CaO:P_2O_5	σ (ohm^{-1}m^{-1}) (10^{-5})	j (eV) (10^{-5})	Φ (eV)	μ (m^{2}V^{1}sec^{-1}) (10^{-13})	N_c (m^{-3}) (10^{26})
10:40:50	4.3	34.2	0.03	27.4	1.0
15:40:45	4.4	25.3	0.03	16.0	1.7
20:40:40	4.5	6.0	0.03	5.7	4.9
25:40:35	5.5	2.1	0.03	3.1	11.1
30:40:30	6.0	1.8	0.03	2.6	14.5

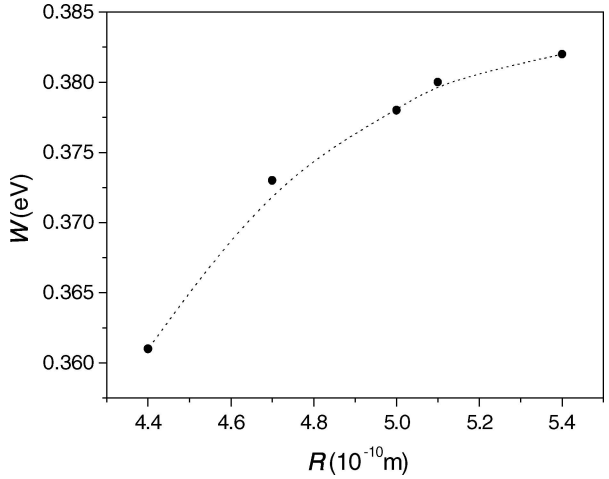

Figure 7 Effect of average ion spacing R on activation energy W for conduction at 400 K for $x\mathrm{V_2O_5}{\cdot}40\mathrm{CaO}{\cdot}(60-x)\mathrm{P_2O_5}$ glasses.

At low temperatures, the polaron binding energy becomes lower than the disorder energy W_d and hence it is reasonable to assume that $W_o = W_d$ [11, 21]. Based on this assumption, the Mott parameters were calculated and tabulated in Table IV.

Both$N(E_F)$ and R_{VRH} vary as a function of $\mathrm{V_2O_5}$ mol%. Fig. 8 shows the variation of $N(E_F)$ and R_{VRH} with change in $\mathrm{V_2O_5}$ mol%. While $N(E_F)$ increases with increase in $\mathrm{V_2O_5}$ mol%, R_{VRH} decreases as the $\mathrm{V_2O_5}$ mol% increases. The increase in $N(E_F)$ and decrease in R_{VRH} are as per the theoretical prediction [17, 22] and agrees with reported behaviour [11] of $\mathrm{V_2O_5}$ based glasses. It is obvious from Fig. 8 that both $N(E_F)$ and R_{VRH} show a slope change at the $x = 20$ mol% $\mathrm{V_2O_5}$ composition. It has already been pointed out that the carrier reversal occurs whenever V^{4+} or V^{5+} ion concentration exceeds the other. Since the d.c electrical conduction mechanism is principally due to electron hopping from a V^{4+} site to V^{5+} site, it is not

TABLE IV Density of states at Fermi energy $N(E_F)$, variable range hopping distance R_{VRH} and disorder energy W_d

Composition (mol%) $\mathrm{V_2O}$:$_5$CaO:$\mathrm{P_2O_5}$	$N(E_F)$ ($\mathrm{m^{-3}eV^{-1}}$) (10^{26})	R_{VRH} (m) (10^{-9})	$\alpha\, R_{\mathrm{VRH}}$	W_d (eV)
10:40:50	1.7	3.84	1.86	0.03
15:40:45	2.1	3.75	1.64	0.03
20:40:40	2.4	3.66	1.51	0.03
25:40:35	3.5	3.46	1.22	0.02
30:40:30	3.9	3.41	1.16	0.02

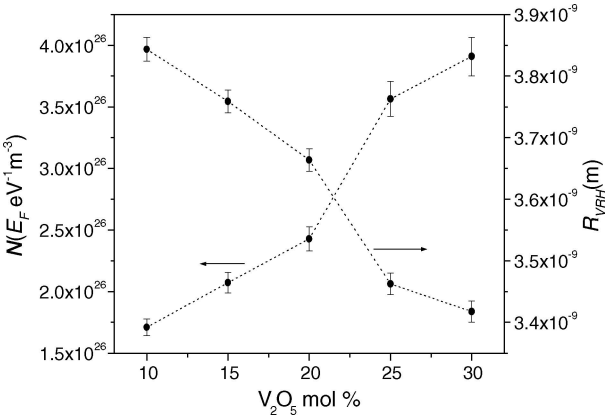

Figure 9 Variation of density of states at Fermi energy $N(E_F)$ and variable range hopping distance (R_{VRH}) with $\mathrm{V_2O_5}$ mol% for $x\mathrm{V_2O_5}{\cdot}40\mathrm{CaO}{\cdot}(60-x)\mathrm{P_2O_5}$ glasses.

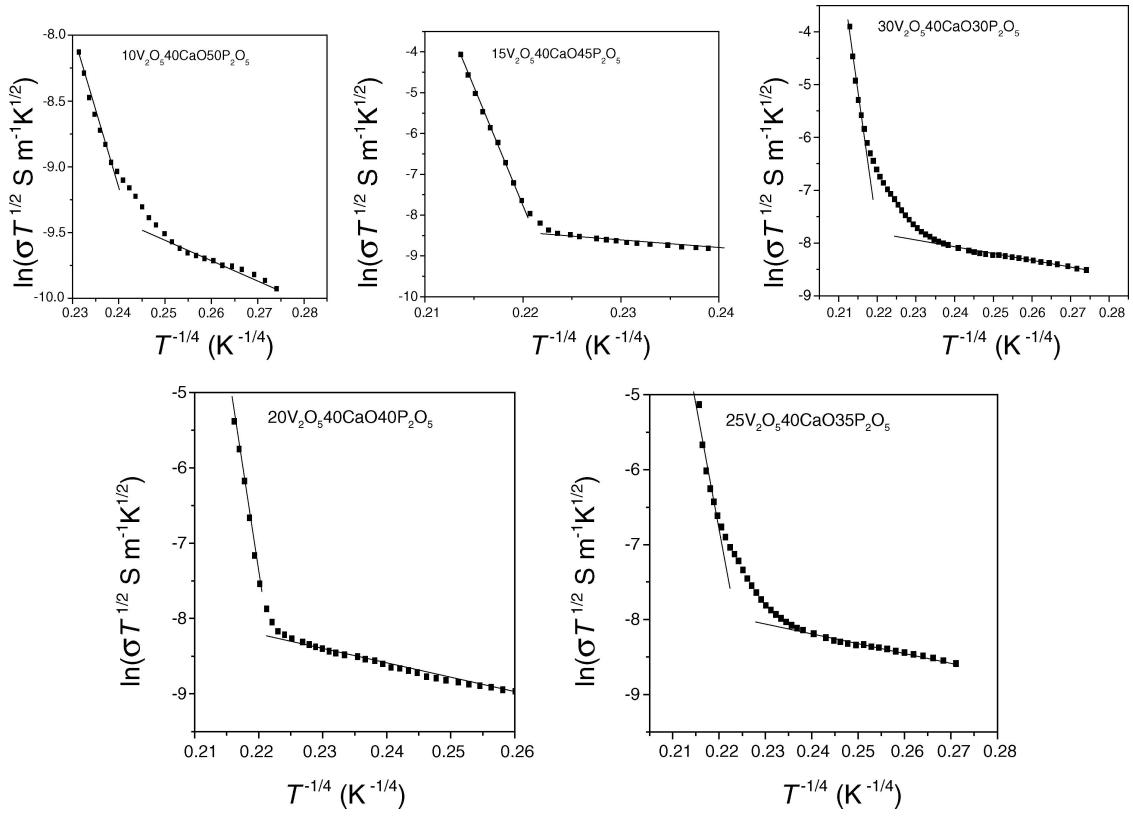

Figure 8 $\ln(\sigma T^{1/2})$ verses $T^{-1/4}$ plots for various compositions of $x\mathrm{V_2O_5}{\cdot}40\mathrm{CaO}{\cdot}(60-x)\mathrm{P_2O_5}$ glasses (Every tenth data point has been plotted in order to improve the clarity of the figure).

surprising for the Mott parameters to carry the signature of the carrier reversal phenomenon in their composition dependence.

4. Conclusion

Glasses with $x = 10$ and 15 mol% V_2O_5 showed p-type conduction and glasses with $x = 25$ and 30 V_2O_5 mol% exhibited n-type conduction in the of $xV_2O_5{\cdot}40CaO{\cdot}(60 - x)P_2O_5$ $(10 \leq x \leq 30)$ glasses. Majority charge carrier reversal occurred at the glass composition with $x = 20$ mol% V_2O_5. The carrier type depends on the relative predominance of V^{4+} or V^{5+} ions. Thus, n-type semiconductors were obtained for glasses for with $(V^{5+}/V^{4+}) > 1$ and vice versa. These glasses exhibited a poor Q dependence on temperature. The activation energy for thermoelectric power ΔE_s, showed a subtle slope change at the composition at which the p-type to n-type transition occurred.

The d.c. electrical conduction mechanism in the high temperature regime is attributed to non-adiabatic small polaron hopping in these glasses. All the glasses showed a changeover from SPH toVRH conduction mechanism when cooled below room temperature. The density of states at fermi energy $N(E_F)$ increased and variable range hopping distance R_{VRH} decreased as V_2O_5 mol% is increased. $N(E_F)$ and R_{VRH} showed a subtle slope change in their values at the composition at which the majority charge carrier reversal occurs in these glasses.

Acknowledgements

Financial support from the Council of Scientific and Industrial Research, Government of India through project # 03(0987)/03/EMR-II is gratefully acknowledged.

References

1. E. P. DENTON, H. RAWSON and J. E. STANWORTH, *Nature* **173** (1954) 1030.
2. T. N. KENNEDY and J. D. MACKENZIE, *Phys. Chem. Glass.* **8** (1967) 169.
3. A. MANSINGH and A. DHAWAN, *J. Phys. C: Solid State Phys.* **11** (1978) 3439.
4. C. H. CHUNG, J. D. MACKENZIE and L. MURAWSKI, *Rev. Chim. Miner.* **16** (1979) 308.
5. L. MURAWSKI, C. H. CHUNG and J. D. MACKENZIE, *J. Non-Cryst. Solids* **32** (1979) 91.
6. H. MORI, J. IGARASHI and H. SAKATA, *J. Ceram. Soc. Jpn*. **101** (1993) 1351.
7. N. F. MOTT, *Adv. Phys.* **16** (1967) 49.
8. *Idem.*, *J. Non-Cryst. Solids* **1** (1968) 1.
9. I. G. AUSTIN and N. F. MOTT, *Adv. Phys.* **18** (1969) 41.
10. A. GHOSH and B. K. CHAUDHURI, *J. Non-Cryst. Solids* **83** (1986) 151.
11. H. MORI, K. GOTOH and H. SAKATA, *ibid.* **183** (1995) 122.
12. S. MANDAL and A. GHOSH, *Phys. Rev. B* **49** (1994) 3131.
13. V. K. DHAWAN and A. MANSINGH, *J. Non-Cryst. Solids* **51** (1982) 87.
14. B. INDRAJIT SHARMA, A. K. PATTANAIK and A. SRINIVASAN, 2001 Proc. 6th ATPC Guwahati University, India.
15. A. K. PATTANAIK, C. BORGOHAIN and A. SRINIVASAN, *Ind. J. Phys.* **74A** (2000) 307.
16. P. C. PAUL, Ph.D thesis 1992, NEHU.
17. S. R. ELLIOT, "Physics of Amorphous Materials" (Longman London, 1984).
18. R. R. HEIKES, in "Thermoelectricity", edited by R. R. Heikes and R. W. Ure, Interscience (1961) p. 81.
19. R. R. HEIKES, A. A MARADUDIN and R. C. MILLER, *Ann. Phys.NY* **8** (1963) 733.
20. J. APPEL, *Solid State Phys.* **21** (1968) 193.
21. J. ZARZYCKI, "Materials Science and Technology" (Weinheim, New York, 1991) Vol. 9.
22. P. NAGELS, in "Amorphous Semiconductors," edited by M. H. Brodsky, 2nd edn. (Springer-Verlag, New York, 1985).
23. B. INDRAJIT SHARMA and A. SRINIVASAN, *Physica Status Solidi b* **229** (2002) 1405.
24. M. AMANO, H. SAKATA, K. TANAKA and T. HIRAYAMA, *J. Ceram. Soc. Jpn.* **102** (1994) 424.
25. T. HOLSTEIN, *Am. Phys. NY* **8** (1959) 34.
26. H. MORI, T. KITAMI and H. SAKATA, *J. Non-Cryst. Solids* **168** (1994)157.
27. N. TOGHE, Y. YAMAMOTO, T. MINAMI and M. TANAKA, *Appl. Phys. Lett*. **34** (1979) 640.
28. H. MORI and H. SAKATA, *J. Ceram. Soc. Jpn*.**102** (1994) 560.

Received 12 December 2002
and accepted 5 November 2004